J. Fluid Mech. (1978), *vol.* 88, *part* 2, *pp.* 241–258
Printed in Great Britain

On the nature of unsteady three-dimensional laminar boundary-layer separation

By JAMES C. WILLIAMS
Department of Mechanical and Aerospace Engineering,
North Carolina State University, Raleigh

(Received 19 December 1977)

Solutions have been obtained for a family of unsteady three-dimensional boundary-layer flows which approach separation as a result of the imposed pressure gradient. These solutions have been obtained in a co-ordinate system which is moving with a constant velocity relative to the body-fixed co-ordinate system. The flows studied are those which are steady in the moving co-ordinate system. The boundary-layer solutions have been obtained in the moving co-ordinate system using the technique of semi-similar solutions. The behaviour of the solutions as separation is approached has been used to infer the physical characteristics of unsteady three-dimensional separation.

In the numerical solutions of the three-dimensional unsteady laminar boundary-layer equations, subject to an imposed pressure distribution, the approach to separation is characterized by a rapid increase in the number of iterations required to obtain converged solutions at each station and a corresponding rapid increase in the component of velocity normal to the body surface. The solutions obtained indicate that separation is best observed in a co-ordinate system moving with separation where streamlines turn to form an envelope which is the separation line, as in steady three-dimensional flow, and that this process occurs within the boundary layer (away from the wall) as in the unsteady two-dimensional case. This description of three-dimensional unsteady separation is a generalization of the two-dimensional (Moore–Rott–Sears) model for unsteady separation.

1. Introduction

The nature of steady two-dimensional laminar boundary-layer separation is well known. Steady two-dimensional separation is characterized by the main flow turning rapidly away from the bounding surface and a region of reverse flow penetrating beneath this main flow. The prominent symptom of separation, in this case, is the vanishing of the wall shear stress.

If either the restriction of steady flow or the restriction of two-dimensional flow is relaxed, the nature of separation becomes considerably more complicated. For unsteady two-dimensional flow, or for steady two-dimensional flow over a moving wall, there is growing evidence that boundary-layer separation is described by the Moore–Rott–Sears model. This model postulates that unsteady separation is characterized by the simultaneous vanishing of the shear stress and the velocity at a point within the boundary layer, as seen by an observer moving with separation. In recent years, a number of numerical solutions have been obtained for laminar boundary-layer flows leading to separation for cases in which separation is moving upstream. These results indicate that the boundary layer remains thin beyond the point of vanishing shear and that separation, in the sense of rapid growth of the viscous layer and a rapid increase in the vertical component of velocity, occurs in the vicinity of the point of simultaneous vanishing of the shear and velocity, as indicated by the Moore–Rott–Sears model. The case in which separation moves downstream remains an enigma. There are no solutions or experimental results as yet which verify the Moore–Rott–Sears model for this case. However, the recent results of Tsahalis (1977) for steady flow over an upstream-moving wall, a problem which is closely related to the problem of unsteady flow with downstream-moving separation, tends to substantiate the Moore–Rott–Sears model.

For steady three-dimensional flow, Maskell (1955) has pointed out that there are two possible modes of separation, modes he terms 'singular' separation and 'ordinary' separation. For 'singular' separation, both components of the wall shear vanish simultaneously. This mode of separation appears to be the exception rather than the rule. On a bluff asymmetric body at an angle of attack, however, singular separation occurs at the two points along the separation line where it crosses the plane of symmetry. Away from these two points, ordinary separation occurs. For ordinary separation, the limiting or 'wall' streamlines run close together to form a line of separation. Ordinary separation appears to be the dominant form of separation on most three-dimensional bodies. Flow-visualization studies (e.g. Peake, Rainbird & Atraghji 1972) and recent numerical computations (Williams 1975) tend to verify the concepts of steady three-dimensional separation advanced by Maskell.

A question quite naturally arises as to the nature of unsteady three-dimensional laminar boundary-layer separation. Is separation in this case a composite of unsteady two-dimensional separation, in which the identifying characteristics occur away from the wall and in a moving co-ordinate system, and steady three-dimensional separation, in which the identifying characteristic is generally streamlines which turn and form an envelope which is the separation line? The present work gives results of an investigation intended to answer, at least partially, this question. Solutions to the unsteady three-dimensional laminar boundary-layer equations are obtained for several cases in which the boundary-layer flow approaches separation and the nature of the solutions in the vicinity of separation is used to infer the nature of unsteady three-dimensional separation.

If the nature of unsteady three-dimensional separation is to be inferred from solutions of the unsteady three-dimensional boundary-layer equations, two serious difficulties must be overcome. The first of these has nothing whatsoever to do with separation; it is simply the practical mathematical problem of obtaining solutions to a set of boundary-layer equations in four independent variables (the three spatial co-ordinates and time). There are available a number of techniques for solving two-dimensional problems and a few techniques for solving problems in three independent variables, but as far as the author can tell, there are no general techniques available for solving boundary-layer problems with four independent variables. This difficulty is overcome in the present work by a combination of a transformation to a moving co-ordinate system and use of the method of semi-similar solutions. In § 2, it is shown that, if the velocity components at the edge of the three-dimensional boundary layer are functions of linear combinations of $\bar{x}$ and $\bar{t}$ and of $\bar{y}$ and $\bar{t}$, then in the appropriate moving co-ordinate system the flow appears as a steady flow over a moving wall. For this class of flows, then, the problem, viewed in the moving co-ordinate system, is a problem in three independent variables (the spatial co-ordinates) and the effect of unsteadiness appears as a parameter (the velocity of the moving wall) rather than as an independent variable. The present analysis is limited to these flows which are steady in the moving co-ordinate system.

Even after the transformation to the moving co-ordinate system, the problem is one in three independent variables. In § 3, the number of independent variables is reduced further by applying the method of semi-similar solutions. Mathematically, this method is a technique which reduces the number of independent variables from three to two by an appropriate scaling. In cases where separation occurs, the technique has a more important physical interpretation. It may be viewed as a scaling of the two surface co-ordinates such that separation occurs at a constant value of the new scaled co-ordinate (although the value of the new scaled co-ordinate corresponding to separation is unknown *a priori*). This property has proved to be extremely helpful in determining, from the solutions, the physical characteristics of separation in the two-dimensional unsteady case (Williams & Johnson 1974) and in the three-dimensional steady case (Williams 1975).

The net result of the two transformations, the transformation to the moving co-ordinate system and the semi-similar transformation, is that the resulting problem is one in two independent variables. The transformed problem may be solved by standard numerical methods which have been shown to be rapid and accurate.

Assuming that solutions may be obtained by the method outlined above, for an unsteady three-dimensional flow which leads to separation one encounters a second and perhaps more serious difficulty. This is the difficulty of identifying three-dimensional unsteady separation. What characteristic features of the boundary layer or the behaviour of the solutions should one look for in order to identify separation? At present, there are neither solutions to the unsteady three-dimensional boundary-layer equations nor experimental investigations which shed light on this problem.

Some indication of what features should be looked for may be obtained by reviewing the features which are found in solutions to other types of flow leading to separation. For two-dimensional steady separation, the generally accepted physical symptom of separation is the vanishing of the wall shear stress. Numerical solutions of the two-dimensional steady boundary-layer equations for flows leading to separation exhibit an increase in the number of iterations required to obtain a converged solution at each station and a rapid increase in the vertical component of velocity as separation is approached (assuming that the external pressure distribution is prescribed). This behaviour is generally accepted as an indication of the Goldstein-type singularity at separation.

For two-dimensional unsteady separation or for two-dimensional steady separation over a moving wall, there is increasing analytical evidence (Sears & Telionis 1975: Telionis 1975; Williams 1977) that the physical symptom of separation is the simultaneous vanishing of the shear stress and the velocity away from the wall in a co-ordinate system moving with separation. Numerical solutions for these flows exhibit an increase in the number of iterations required to obtain a converged solution at each station and a rapid increase in the vertical component of velocity as separation is approached. This behaviour is also believed to be the result of a Goldstein-type singularity at separation, but the nature of this singularity has not been definitely demonstrated.

For three-dimensional steady separation, both analytical and experimental results verify the conclusion of Maskell (1955) that there are two modes of separation: singular separation and ordinary separation. The physical symptom of singular separation is the simultaneous vanishing of both components of the wall shear stress either at a point on the separation line or along the separation line. The physical symptom of ordinary separation is the turning of the wall or limiting streamlines to form an envelope which is the separation line. For both singular and ordinary separation, numerical solutions leading to separation exhibit an increase in the number of iterations required to obtain a converged solution, at each station, and a rapid increase in the vertical component of velocity as separation is approached.

The above discussion clearly indicates that, although the physical symptoms of separation are different for each type of flow, numerical solutions in each case exhibit the same characteristics. In the numerical solutions separation is heralded by (i) an increase in the number of iterations required to obtain convergence at each station and (ii) a rapid increase of the vertical component of velocity. It should be pointed out that these two indications are not independent but are probably closely related. The existing evidence suggests that both of these indicators are probably manifestations of a singularity in solutions to the boundary-layer equations at separation. Only in the case of two-dimensional steady flow, however, has the possibility of a mathematical singularity at the separation point been completely verified.

In any event, these common features of numerical solutions to various types of separation suggest a plausible strategy for determining the nature of unsteady three-dimensional laminar boundary-layer separation. Solutions have been obtained, by the methods outlined above, to the unsteady three-dimensional boundary-layer equations for flows which should lead to separation. These solutions and a discussion of their implications are presented in § 4. The solutions were monitored to determine if and when the number of iterations required for convergence and the vertical component of velocity begin to increase rapidly. The occurrence of these events is taken, by analogy with solutions to two-dimensional steady flow, two-dimensional unsteady flow and three-dimensional steady flow, as an indication of impending separation. The physical nature of three-dimensional unsteady laminar boundary-layer separation is inferred from the behaviour of the solutions as separation is approached.

These results indicate that three-dimensional unsteady separation is characterized by the turning of the flow, as seen in a moving co-ordinate system, so that the streamlines form an envelope which is a separation line, as in the steady three-dimensional case, and that this process occurs away from the wall and is best observed in the moving co-ordinate system, as in the unsteady two-dimensional case.

2. Transformation to a moving co-ordinate system

We consider the general three-dimensional unsteady boundary-layer problem for an incompressible constant-property fluid moving over a surface whose radii of curvature are large compared with the thickness of the boundary layer. The boundary-

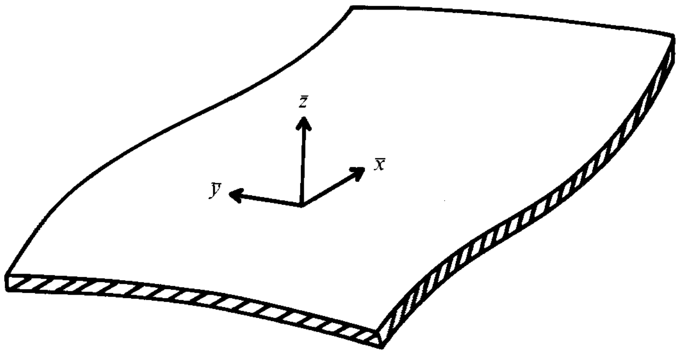

FIGURE 1. Body-fixed boundary-layer co-ordinate system.

layer equations and boundary conditions for this problem, in a rectangular Cartesian co-ordinate system where $\bar{x}$ and $\bar{y}$ are the orthogonal co-ordinates on the surface of the body and $\bar{z}$ is the co-ordinate normal to the body surface (figure 1), are

$$\frac{\partial \bar{u}}{\partial \bar{x}}+\frac{\partial \bar{v}}{\partial \bar{y}}+\frac{\partial \bar{w}}{\partial \bar{z}} = 0, \tag{1}$$

$$\frac{\partial \bar{u}}{\partial \bar{t}}+\bar{u}\frac{\partial \bar{u}}{\partial \bar{x}}+\bar{v}\frac{\partial \bar{u}}{\partial \bar{y}}+\bar{w}\frac{\partial \bar{u}}{\partial \bar{z}} = \frac{\partial \bar{u}_\delta}{\partial \bar{t}}+\bar{u}_\delta\frac{\partial \bar{u}_\delta}{\partial \bar{x}}+\bar{v}_\delta\frac{\partial \bar{u}_\delta}{\partial \bar{y}}+\nu\frac{\partial^2 \bar{u}}{\partial \bar{z}^2}, \tag{2}$$

$$\frac{\partial \bar{v}}{\partial \bar{t}}+\bar{u}\frac{\partial \bar{v}}{\partial \bar{x}}+\bar{v}\frac{\partial \bar{v}}{\partial \bar{y}}+\bar{w}\frac{\partial \bar{v}}{\partial \bar{z}} = \frac{\partial \bar{v}_\delta}{\partial \bar{t}}+\bar{u}_\delta\frac{\partial \bar{v}_\delta}{\partial \bar{x}}+\bar{v}_\delta\frac{\partial \bar{v}_\delta}{\partial \bar{y}}+\nu\frac{\partial^2 \bar{v}}{\partial \bar{z}^2}, \tag{3}$$

$$\left.\begin{aligned}&\bar{u}(\bar{x},\bar{y},0,\bar{t}) = \bar{v}(\bar{x},\bar{y},0,\bar{t}) = \bar{w}(\bar{x},\bar{y},0,\bar{t}) = 0,\\ &\lim_{\bar{z}\to\infty} u(\bar{x},\bar{y},\bar{z},\bar{t}) = u_\delta(\bar{x},\bar{y},\bar{t}), \quad \lim_{\bar{z}\to\infty} v(\bar{x},\bar{y},\bar{z},\bar{t}) = v_\delta(\bar{x},\bar{y},\bar{t}).\end{aligned}\right\} \tag{4}$$

Here $\bar{u}$, $\bar{v}$ and $\bar{w}$ are the velocity components in the $\bar{x}$, $\bar{y}$ and $\bar{z}$ directions, respectively.

We wish, however, to examine the flow in a moving co-ordinate system with co-ordinates x, y and z parallel to $\bar{x}$, $\bar{y}$ and $\bar{z}$, respectively. The velocity components in the moving (x, y, z) co-ordinate system are denoted by u, v and w, respectively. This new, moving co-ordinate system is assumed to be moving parallel to the x axis with a velocity $\bar{U}(t)$ and parallel to the $\bar{y}$ axis with a velocity $\bar{V}(t)$. The relationships between the fixed and moving co-ordinates and between the velocity components in these co-ordinate systems are

$$\bar{x} = x+\int \bar{U}(\bar{t})\,d\bar{t}, \quad \bar{y} = y+\int \bar{V}(\bar{t})\,d\bar{t}, \quad z = \bar{z}, \quad t = \bar{t},$$
$$\bar{u} = u+\bar{U}, \quad \bar{v} = v+\bar{V}, \quad w = \bar{w},$$

where the overbars refer to the fixed co-ordinate system. In the moving co-ordinate system the boundary-layer equations and the corresponding boundary conditions become

$$\frac{\partial u}{\partial x}+\frac{\partial v}{\partial y}+\frac{\partial w}{\partial z} = 0, \tag{5}$$

$$\frac{\partial u}{\partial t}+u\frac{\partial u}{\partial x}+v\frac{\partial u}{\partial y}+w\frac{\partial u}{\partial z} = \frac{\partial u_\delta}{\partial t}+u_\delta\frac{\partial u_\delta}{\partial x}+v_\delta\frac{\partial u_\delta}{\partial y}+\nu\frac{\partial^2 u}{\partial z^2}, \tag{6}$$

$$\frac{\partial v}{\partial t}+u\frac{\partial v}{\partial x}+v\frac{\partial v}{\partial y}+w\frac{\partial v}{\partial z}=\frac{\partial v_\delta}{\partial t}+u_\delta\frac{\partial v_\delta}{\partial x}+v_\delta\frac{\partial v_\delta}{\partial y}+\nu\frac{\partial^2 v}{\partial z^2}, \tag{7}$$

$$\left.\begin{aligned}&u(x,y,0,t)=-\bar{U},\quad v(x,y,0,t)=-\bar{V},\quad w(x,y,0,t)=0,\\&\lim_{z\to\infty}u(x,y,z,t)=\bar{u}_\delta(\bar{x},\bar{y},\bar{t})-\bar{U}(t)=u_\delta(x,y,t),\\&\lim_{z\to\infty}v(x,y,z,t)=\bar{v}_\delta(\bar{x},\bar{y},\bar{t})-\bar{V}(t)=v_\delta(x,y,t).\end{aligned}\right\} \tag{8}$$

We now note that, if the external velocity distributions in the fixed co-ordinate system are functions only of linear combinations of $\bar{x}$ and $\bar{t}$ and of $\bar{y}$ and $\bar{t}$, i.e.

$$\bar{u}_\delta(\bar{x}\ \bar{y},\bar{t})=f_1(a\bar{x}+b\bar{t},c\bar{y}+d\bar{t}),\quad \bar{v}_\delta(\bar{x},\bar{y},\bar{t})=f_2(a\bar{x}+b\bar{t},c\bar{y}+d\bar{t}),$$

and if the relative velocity $[\bar{U}(t),\ \bar{V}(t)]$ of the two co-ordinate systems is constant, the external velocity distributions in the moving co-ordinate system are

$$u_\delta(x,y,t)=f_1(ax+a\bar{U}t+bt,cy+c\bar{V}t+dt)-\bar{U},$$

$$v_\delta(\bar{x},\bar{y},\bar{t})=f_2(ax+a\bar{U}t+bt,cy+c\bar{V}t+dt)-\bar{V}.$$

If the relative velocity $\bar{U}$ is taken as $-b/a$ and the relative velocity $\bar{V}$ is taken as $-d/c$ we obtain

$$u_\delta(x,y,t)=f_1(ax,cy)+b/a,\quad v_\delta(x,y,t)=f_2(ax,cy)+d/c$$

and

$$u(x,y,0,t)=+b/a,\quad v(x,y,0,t)=+c/d.$$

Thus, in the moving co-ordinate system, the external velocities are independent of time and the wall boundary conditions are constant, so that the problem posed above is steady. We now limit our consideration to those problems which are steady in the moving co-ordinate system.

3. The semi-similar transformation

Even in this case, where the flow is steady in the moving co-ordinate system, there are still three independent variables (x,y,z) and the boundary-layer problem is difficult. To make the problem tractable, we use the method of semi-similar solutions (Williams 1975) to reduce the number of independent variables further. We introduce the new independent variables η and ξ defined by

$$\eta=z/\nu^{\frac{1}{2}}g(x,y),\quad \xi=\xi(x,y)$$

and introduce a pair of functions $F(\xi,\eta)$ and $G(\xi,\eta)$ defined such that

$$\left.\begin{aligned}&u=u_\delta\,\partial F(\xi,\eta)/\partial\eta,\quad v=v_\delta\,\partial G(\xi,\eta)/\partial\eta,\\&w=-\nu^{\frac{1}{2}}\left\{F\frac{\partial}{\partial x}u_\delta g+u_\delta g\frac{\partial\xi}{\partial x}\frac{\partial F}{\partial\xi}-u_\delta\frac{\partial g}{\partial x}\eta\frac{\partial F}{\partial\eta}\right.\\&\qquad\left.+G\frac{\partial}{\partial y}v_\delta g+v_\delta g\frac{\partial\xi}{\partial y}\frac{\partial G}{\partial\xi}-v_\delta\frac{\partial g}{\partial y}\eta\frac{\partial G}{\partial\eta}\right\}.\end{aligned}\right\} \tag{9}$$

It is easily shown by direct substitution that this choice satisfies the continuity equation. If the velocity components given by (9) and their derivatives are introduced into the x and y momentum equations (6) and (7) and it is remembered that in this co-ordinate system the flow is steady, one obtains the following pair of coupled partial differential equations in the two variables η and ξ:

$$\frac{\partial^3 F}{\partial \eta^3}+(A+B)F\frac{\partial^2 F}{\partial \eta^2}+(C+D)G\frac{\partial^2 F}{\partial \eta^2}+A\left[1-\left(\frac{\partial F}{\partial \eta}\right)^2\right]+E\left(1-\frac{\partial F}{\partial \eta}\frac{\partial G}{\partial \eta}\right)$$
$$+H\left(\frac{\partial^2 F}{\partial \eta^2}\frac{\partial F}{\partial \xi}-\frac{\partial F}{\partial \eta}\frac{\partial^2 F}{\partial \xi \partial \eta}\right)+I\left(\frac{\partial^2 F}{\partial \eta^2}\frac{\partial G}{\partial \xi}-\frac{\partial G}{\partial \eta}\frac{\partial^2 F}{\partial \xi \partial \eta}\right)=0, \quad (10)$$

$$\frac{\partial^3 G}{\partial \eta^3}+(C+D)G\frac{\partial^2 G}{\partial \eta^2}+(A+B)F\frac{\partial^2 G}{\partial \eta^2}+C\left[1-\left(\frac{\partial G}{\partial \eta}\right)^2\right]+J\left(1-\frac{\partial F}{\partial \eta}\frac{\partial G}{\partial \eta}\right)$$
$$+I\left(\frac{\partial^2 G}{\partial \eta^2}\frac{\partial G}{\partial \xi}-\frac{\partial G}{\partial \eta}\frac{\partial^2 G}{\partial \xi \partial \eta}\right)+H\left(\frac{\partial^2 G}{\partial \eta^2}\frac{\partial F}{\partial \xi}-\frac{\partial F}{\partial \eta}\frac{\partial^2 G}{\partial \xi \partial \eta}\right)=0. \quad (11)$$

In the transformed co-ordinate system, the boundary conditions become

$$\left.\begin{array}{c} F(\xi,0)=G(\xi,0)=0, \\ \partial F(\xi,0)/\partial\eta = b/(a\,u_\delta(x,y)), \quad \partial G(\xi,0)/\partial\eta = c/(d\,v_\delta(x,y)), \\ \lim\limits_{\eta\to\infty}\partial F(\xi,\eta)/\partial\eta = 1, \quad \lim\limits_{\eta\to\infty}\partial G(\xi,\eta)/\partial\eta = 1. \end{array}\right\} \quad (12)$$

In the above equations the coefficients A, B, C, D, E, H, I and J are functions of x and y given by

$$A(\xi) = g^{*2}\,\partial u_\delta^*/\partial x^*, \quad B(\xi) = \tfrac{1}{2}u_\delta^*\,\partial g^{*2}/\partial x^*, \quad (13a,b)$$

$$C(\xi) = g^{*2}\frac{\partial v_\delta^*}{\partial y^*}, \quad D(\xi) = \tfrac{1}{2}v_\delta^*\,\partial g^{*2}/\partial y^*, \quad (13c,d)$$

$$E(\xi) = g^{*2}\frac{v_\delta^*}{u_\delta^*}\frac{\partial u_\delta^*}{\partial y^*}, \quad J(\xi) = g^{*2}\frac{u_\delta^*}{v_{\delta *}}\frac{\partial v_\delta^*}{\partial x^*}, \quad (13e,f)$$

$$H(\xi) = g^{*2}u_\delta^*\frac{\partial \xi}{\partial x^*}, \quad I(\xi) = g^{*2}v_\delta^*\frac{\partial \xi}{\partial y^*}. \quad (13g,h)$$

In (13), u_δ, v_δ, g, x and y have been normalized by introducing the dimensionless variables

$$u_\delta^* = \frac{u_\delta}{U_\infty}, \quad v_\delta^* = \frac{v_\delta}{U_\infty}, \quad g^* = g\left(\frac{U_\infty}{l}\right)^{\frac{1}{2}}, \quad x^* = \frac{x}{l}, \quad y^* = \frac{y}{l},$$

where U_∞ and l are some characteristic velocity and length for the problem under consideration.

If semi-similar solutions are to exist, the coefficients A, B, C, D, E, H, I and J must be functions of ξ alone. There are eight of these coefficients but we may construct four relations among them by noting that u_δ^*, v_δ^*, g^* and ξ must be continuous functions of x^* and y^*. Thus the second derivative of each of these functions with respect to x^* and y^* is independent of the order of differentiation. If ($13a$) is differentiated with respect to y^* and ($13c$) with respect to x^* and the results combined with the definitions (13), one obtains

$$E'H - A'I = -2AD + 2BE + E(J-A). \quad (14a)$$

Similarly, one obtains

$$B'I - D'H = BE - DJ, \tag{14b}$$

$$J'I - C'H = -2BC + J(2D + E - C), \tag{14c}$$

$$I'H - H'I = I(2B + J) - H(2D + E), \tag{14d}$$

where the primes indicate differentiation with respect to ξ.

There are eight coefficients A, B, C, D, E, H, I and J and there are four relations (14a–d) among these coefficients. Thus four of the coefficients may be chosen arbitrarily. In most practical cases, the outer flow is irrotational, so that the component of vorticity normal to the wall vanishes outside the boundary layer, i.e.

$$\partial v_\delta^* / \partial x^* = \partial u_\delta^* / \partial y^*.$$

Imposing this restriction yields an additional relation between two of the coefficients:

$$E = (v_\delta^* / u_\delta^*)^2 J. \tag{15}$$

Thus, if the outer flow is to be irrotational, only three of the eight coefficients may be chosen arbitrarily. Further, since for semi-similar solutions both E and J must be functions of ξ only, the ratio v_δ^*/u_δ^* must be a function of ξ alone if the outer flow is irrotational.

The assumption of an irrotational outer flow imposes a restriction on the shape of lines of constant ξ. The slope of constant-ξ lines in the x, y plane is given by

$$\left.\frac{dx^*}{dy^*}\right|_{\xi=\text{const}} = \frac{\partial \xi}{\partial y^*} \bigg/ \frac{\partial \xi}{\partial x^*} = I(\xi)\, v_\delta^* / H(\xi)\, u_\delta^*.$$

If the outer flow is irrotational then, as noted above, the ratio v_δ^*/u_δ^* is a function of ξ alone and the slope of lines of constant ξ is a function of ξ alone. Hence lines of constant ξ are straight lines in the x, y plane and, if separation occurs, the separation line will be a straight line.

A direct solution to a general three-dimensional boundary-layer problem by the method of semi-similar solutions would be initiated with known velocities $u^*(x,y)$ and $v^*(x,y)$ outside the boundary layer obtained from a solution of the inviscid flow field. With the external velocity distribution known one would then obtain the scaling functions $g(x,y)$ and $\xi(x,y)$ and the coefficients A, B, C, D, E, H and I from (13)–(15). Finally, with all the coefficients known, the solution of (10) and (11) could be obtained by standard numerical methods which are both rapid and accurate. It has been pointed out (Williams 1975), however, that such direct solutions are not possible and that, in fact, a semi-similar transformation does not exist for every possible combination of external velocity distributions. In the present work, we employ an indirect method of solution in which four assumptions are made relating the coefficients given in (13). The additional coefficients are obtained by solving (14) and (15) and finally the external velocities and scaling functions $g(x,y)$ and $\xi(x,y)$ are obtained by solving (13). Once all of the coefficients defined in (13) are known, the solution of (10) and (11) is rather straightforward by modern numerical techniques.

The four assumptions relating the coefficients defined by (13) which are employed in the present analysis are (i) that the outer flow is irrotational, (ii) that the external velocity u_δ^* is a function of ξ alone, specifically $u_\delta^* = 1 - \xi$, (iii) that the coefficients $A(\xi)$ and $B(\xi)$ are related by $A(\xi) + 2B(\xi) = 1$ and (iv) that the coefficient $H(\xi)$ is given by $H(\xi) = \xi$. As noted above, the assumption of irrotational flow implies that lines of constant ξ are straight lines in the x^*, y^* plane. The equations for these straight lines will be determined later. The second assumption, when combined with the first, implies that v_δ^* is also a function of ξ alone. The third assumption leads to the relation $u_\delta^* g^2 = x^*$, which, when combined with the fourth assumption and (13f), yields the result $\xi = x^* m(y^*)$. When this result is used in (13g) one obtains $m(y^*) = 1/(1-\alpha y^*)$, so that the scaling functions $g(x, y)$ and $\xi(x,y)$ become

$$g^2 = x^*/u_\delta^*, \quad \xi = x^*/(1-\alpha y^*)$$

and each of the eight coefficients given by (13) can now be written in terms of $u_\delta^*(\xi)$ and $v_\delta^*(\xi)$. The relationship between $u_\delta^*(\xi)$ and $v_\delta^*(\xi)$ comes from the auxilliary equations (14a–d), which in the present case reduce to the single equation

$$v_\delta^*(\xi) = \alpha \int_0^\xi \xi \frac{du_\delta^*}{d\xi} d\xi + C_1,$$

where C_1 is a constant of integration. In the present case, with the assumed form of u_δ^* we obtain

$$v_\delta^* = 1 - \tfrac{1}{2}\alpha\xi^2.$$

In summary then, we have for the present analysis

$$u_\delta^* = 1-\xi, \quad v_\delta^* = 1 - \tfrac{1}{2}\alpha\xi^2, \tag{16), (17}$$

$$\xi = x^*/(1-\alpha y^*), \quad g^2 = x^*/u_\delta^* \tag{18), (19}$$

and the coefficients defined by (13) become

$$A(\xi) = -\xi/(1-\xi), \quad B(\xi) = \tfrac{1}{2}(1-A(\xi)), \quad C(\xi) = -\alpha^2\xi^2 A(\xi),$$

$$D(\xi) = \alpha^2\xi^2(1-\tfrac{1}{2}\alpha\xi^2)/(2(1-\xi)^2), \quad E(\xi) = -D(\xi), \quad H(\xi) = \xi,$$

$$I(\xi) = \alpha\xi^2(1-\tfrac{1}{2}\alpha\xi^2)/(1-\xi), \quad J(\xi) = -\alpha\xi^2/(1-\tfrac{1}{2}\alpha\xi^2).$$

It is noted that the x^* component u_δ^* of the external velocity is linearly retarded in the x^* direction at a rate which increases with y^* if α is positive and decreases with y^* if α is negative. The y^* component v_δ^* of the external velocity is uniform if α is zero, decreases with increasing x^* or decreasing y^* if α is positive and increases with increasing x^* or decreasing y^* if α is negative. The non-dimensional pressure gradients in the x^* and y^* directions, as seen by an observer in the moving co-ordinate system, are

$$\frac{g^2}{u_\delta^*}\frac{\partial p^*}{\partial x^*} = +\xi/(1-\xi) + \alpha^2\xi^2(1-\tfrac{1}{2}\alpha\xi^2)/2(1-\xi)^2, \tag{20}$$

$$\frac{g^2}{v_\delta^*}\frac{\partial p^*}{\partial y^*} = -\alpha^2\xi^3/(1-\xi) + \alpha\xi^2/(1-\tfrac{1}{2}\alpha\xi^2). \tag{21}$$

The pressure gradient in the x^* direction is always positive, but the pressure gradient in the y^* direction depends upon both the value of α and the value of ξ.

The physical significance of the parameter α is now clear. If $\alpha = 0$, we have a linearly retarded outer flow in the x direction with a corresponding pressure gradient in the x direction and a uniform outer flow in the y direction. This corresponds to the flow over a certain infinite cylinder and the boundary-layer development may be treated

α	$\bar{U}$	$\bar{V}$	ξ_{sep}	β_{max} at ξ_{sep}	β_{sep}
1	0·2	0·2	0·3062	1·849	1·868
0·8	0·2	0·2	0·3062	1·777	1·811
0·6	0·2	0·2	0·3049	1·718	1·752
0·4	0·2	0·2	0·3023	1·662	1·691
0·2	0·2	0·2	0·2984	1·601	1·630
0·0	0·2	0·2	0·2934	1·562	1·571
−0·2	0·2	0·2	0·2875	1·482	1·513
−0·4	0·2	0·2	0·2810	1·440	1·459
−0·6	0·2	0·2	0·2739	1·391	1·408
−0·8	0·2	0·2	0·2666	1·342	1·360
−1·0	0·2	0·2	0·2590	1·307	1·317
1·0	0·4	0·2	0·480	1·998	2·018
1·0	0·6	0·2	0·6459	2·083	2·144
1·0	0·2	0·4	0·3399	1·878	1·898
1·0	0·2	0·6	0·3799	1·917	1·934

TABLE 1

by the theory of Sears (1948). If α is non-zero, then the outer flow in the y direction is not uniform and a pressure gradient in the y direction arises. This alters the pressure gradient in the x direction because the outer flow is irrotational. The parameter α, then, is a measure of the non-uniformity of the outer flow or, more specifically, a measure of the pressure gradient in the y direction.

4. Solutions and their implications

The problem of determining the characteristics of the laminar three-dimensional unsteady boundary layer for the external flow represented, in the moving co-ordinate system, by (16) and (17) has now been reduced to that of obtaining solutions to (10) and (11) subject to the boundary conditions given by (12) and with the prescribed variation of the coefficients $A(\xi)$, $B(\xi)$, $C(\xi)$, $D(\xi)$, $E(\xi)$, $H(\xi)$, $I(\xi)$ and $J(\xi)$. As long as the coefficient $H(\xi)F'(\xi,\eta)+I(\xi)G'(\xi,\eta)$ is positive, (10) and (11) form a pair of coupled well-posed parabolic partial differential equations. Solutions have been obtained for a number of values of the parameter α, which is a measure of the pressure gradient in the y direction, and for various combinations of $\bar{U}$ and $\bar{V}$, which, in the present case, are a measure of the unsteadiness in the original flow. The values of α, $\bar{U}$ and $\bar{V}$ for which solutions have been calculated are indicated in table 1. These solutions were obtained using an implicit finite-difference technique similar in detail to that of Blottner (1970). In this technique, the solution starts at $\xi = 0$, where the solution is similar, and proceeds in the direction of increasing ξ. The ξ derivatives are represented by two-point backward differences at the second station and by three-point backward differences at subsequent stations. The resulting finite-difference equations at each station are nonlinear, but are treated as linear equations in which the coefficients are updated after each iteration. The iteration process at each ξ station is repeated until the velocity profiles, for two successive iterations, agree to within a prescribed small tolerance.

In some of the cases investigated, one of the normalized velocity components

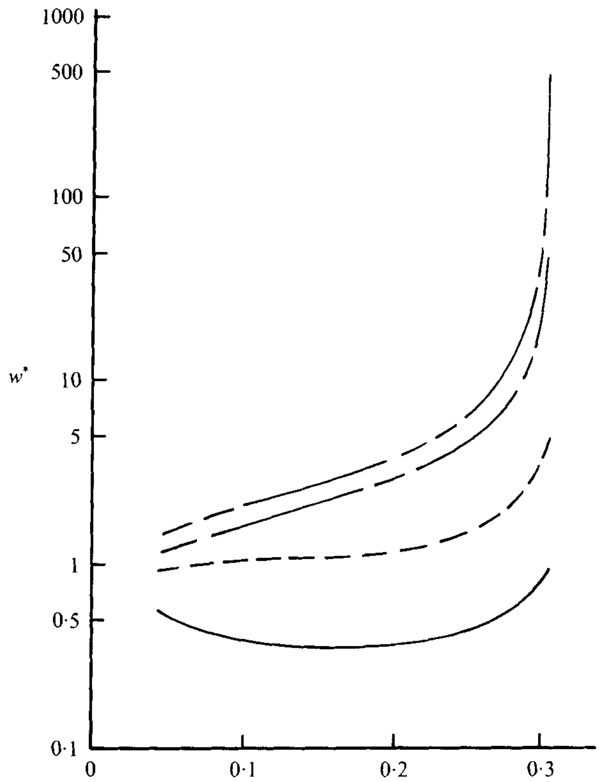

FIGURE 2. Variation of normal velocity component with ξ; $\alpha = 1$, $\bar{U} = \bar{V} = 0{\cdot}2$. ——, $z^* = 0{\cdot}5704$; – – –, $z^* = 1{\cdot}0898$; — —, $z^* = 2{\cdot}1664$; —– —–, $z^* = 3{\cdot}5039$.

$F'(\xi, \eta)$ or $G'(\xi, \eta)$ becomes negative and the numerical integration proceeds into a region of reverse flow (for one velocity component). It has been pointed out (Williams 1977) that integration into regions of reverse flow of one of the velocity components is permissible, provided that the coefficient $H(\xi)\,F'(\xi, \eta) + I(\xi)\,G'(\xi, \eta)$ remains positive. In all the solutions obtained in the present work, this coefficient was positive.

In the present investigation, we have considered only cases where $\bar{U}$ and $\bar{V}$ are both positive. If separation occurs, these flows represent flows in which separation moves forwards along the body. In the moving co-ordinate system, the separation is stationary and the wall moves downstream (in the $+\bar{x}$ and $+\bar{y}$ directions) with respect to separation. The cases in which $\bar{U}$ and $\bar{V}$ are both negative correspond to flows in which the separation moves downstream relative to the fixed wall or, in the moving co-ordinate system, the wall moves upstream relative to separation. With $\bar{U}$ and $\bar{V}$ both negative, the coefficient $H(\xi)\,F'(\xi, \eta) + I(\xi)\,G'(\xi, \eta)$ is generally negative near the wall, so that (10) and (11) become ill-posed parabolic equations. Numerical solutions for such equations are not possible at this time. The interesting case in which $\bar{U}$ and $\bar{V}$ are of opposite sign, which corresponds to a rotating separation line over a fixed wall or, in the moving co-ordinate system, to a rotating wall beneath a stationary separation line, has not been considered here.

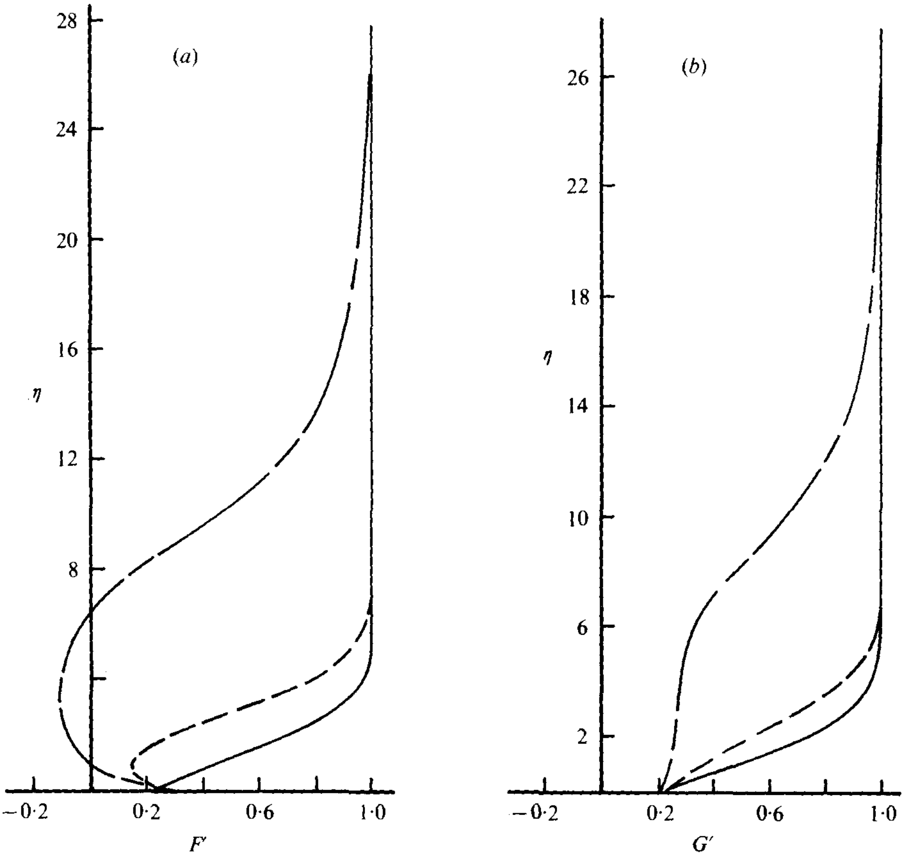

FIGURE 3. Profiles of (a) the x and (b) the y component of velocity in the moving co-ordinate system; $\alpha = 1$, $\bar{U} = \bar{V} = 0{\cdot}2$. ——, $\xi = 0{\cdot}095$; – – –, $\xi = 0{\cdot}275$; — —, $\xi = 0{\cdot}3062$.

Since each of the solutions obtained had the same general characteristics, only the results obtained for the case $\alpha = 1$, $\bar{U} = \bar{V} = 0{\cdot}2$ will be presented here in detail. In this case, as in others, the solution was started at $\xi = 0$ and proceeded in the direction of increasing ξ. At each ξ station, iteration was required to obtain a converged velocity profile. For small ξ, the number of iterations required to obtain convergence was rather small (6 iterations for $\xi = 0{\cdot}05$, 8 iterations for $\xi = 0{\cdot}186$, etc.). At $\xi = 0{\cdot}235$, the number of iterations required for convergence began to grow slowly (9 iterations for $\xi = 0{\cdot}235$, 12 iterations for $\xi = 0{\cdot}303$) and finally, at approximately $\xi = 0{\cdot}3060$, the number of iterations required for convergence began to increase rapidly (16 iterations at $\xi = 0{\cdot}3060$, 18 iterations at $\xi = 0{\cdot}3061$, 24 iterations at $\xi = 0{\cdot}3062$). It was not possible to obtain a solution at $\xi = 0{\cdot}3063$ in what was deemed to be a reasonable number of iterations (120). The rapid increase in the number of iterations required for convergence as ξ approaches $\xi = 0{\cdot}3063$ is accompanied by a rapid increase in the vertical component of velocity

$$w^* = \frac{w}{u_\delta}\left(\frac{u_\delta x}{\nu}\right)^{\frac{1}{2}},$$

particularly in the outer portions of the boundary layer. This behaviour is indicated in figure 2, which shows, for example, that for

$$z^* = z(U/\nu l)^{\frac{1}{2}} = 3{\cdot}5039,$$

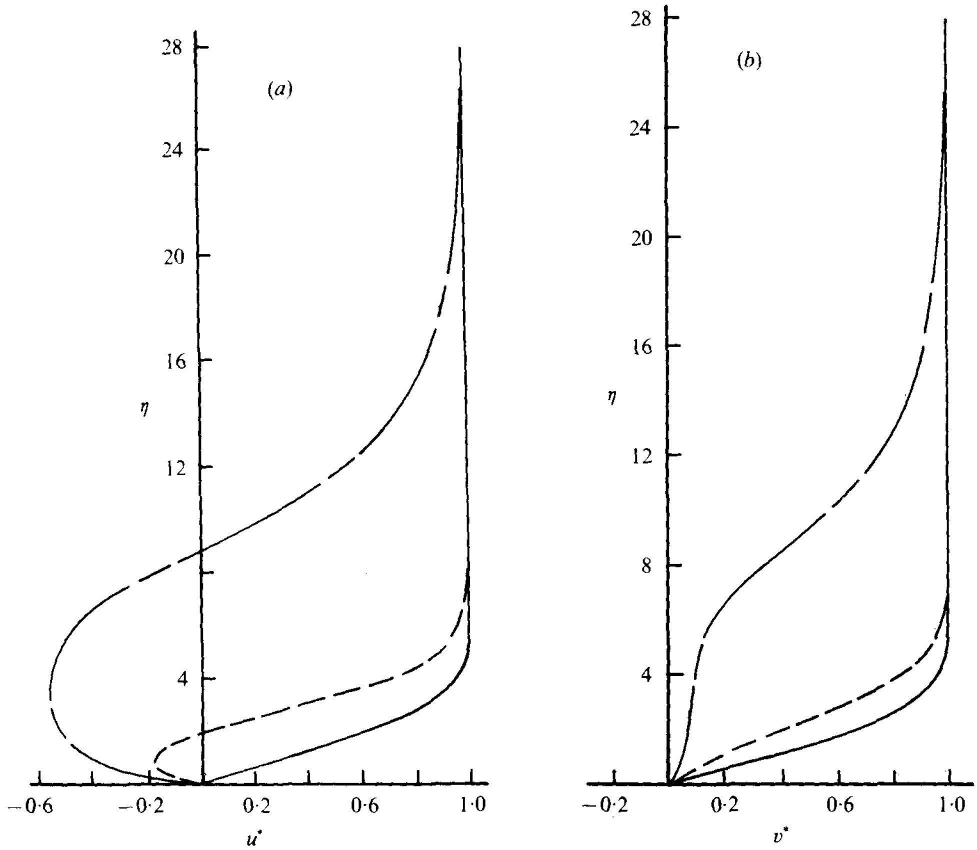

FIGURE 4. Profiles of (*a*) the x and (*b*) the y component of velocity in the fixed co-ordinate system; $\alpha = 1$, $\bar{U} = \bar{V} = 0\cdot2$. ——, $\xi = 0\cdot095$; – – –, $\xi = 0\cdot275$; —–, $\xi = 0\cdot3062$.

w^* increases by a factor of 100 between $\xi = 2\cdot5$ and $\xi = 3\cdot062$. The combination of a rapid increase in the number of iterations required for convergence and a rapid increase in the vertical component of velocity is taken, as explained earlier, as an indication of the approach of boundary-layer separation.

The question now is: what are the physical characteristics of separation? A hint as to what these characteristics are may be obtained from the velocity profiles. Figures 3 (*a*) and (*b*) show the normalized velocity profiles for the x and y components of velocity respectively, for several values of ξ, as seen in the moving co-ordinate system. The corresponding velocity profiles in the fixed co-ordinate system are shown in figures 4 (*a*) and (*b*), respectively. In the present case ($\alpha = 1$) the pressure gradients in both the x and the y direction are positive for $0 \leqslant \xi \leqslant 0\cdot3063$. The pressure gradient in the x direction is, however, much greater than that in the y direction. As a result, the x component of momentum is depleted much more rapidly than the y component of momentum in the lower region of the boundary layer, and the x component of velocity u decreases and finally reverses, while the y component of velocity is reduced but not reversed. We note that the x component of velocity is reversed in both the moving and the fixed co-ordinate system and that these regions of reverse flow were obtained without computational difficulties for the reason mentioned earlier.

The large changes in the x component of velocity accompanied by relatively small

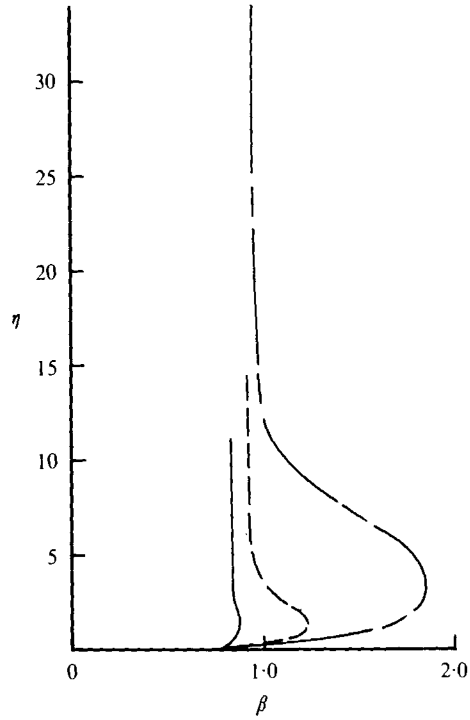

FIGURE 5. Variation of flow deflexion angle β with η for several values of ξ; $\alpha = 1$, $\bar{U} = \bar{V} = 0{\cdot}2$. ——, $\xi = 0{\cdot}095$; – – –; $\xi = 0{\cdot}275$; — –, $\xi = 0{\cdot}3062$.

changes in the y component of velocity give rise to relatively large changes in the flow direction. The projection of the velocity vector on the plane $z = 0$ makes an angle β with the x axis, where

$$\beta = \arctan(v/u) = \arctan(v_\delta G'/u_\delta F').$$

The variation of β with η is presented in figure 5 for the values of ξ for which velocity profiles are shown. As η is increased from zero, β increases, reaches a maximum near the wall, then decreases again for large η. Further, this maximum increases in magnitude as separation is approached because of the rapid depletion of x momentum. The value of β at the wall in this system (where the wall is moving) is given by

$$\beta_w = \arctan(\bar{V}/\bar{U}).$$

For the case presented in figure 5, $\beta_w = 0{\cdot}7854$ independent of ξ.

Now for three-dimensional steady separation there is a maximum (or minimum) flow angle β, which occurs at the wall. This is the angle of the so-called limiting streamlines. As ordinary steady three-dimensional separation is approached, the angle of the limiting streamlines increases (or decreases) rapidly to approach the angle of the separation line, indicating limiting streamlines which become tangential to the separation line (Williams 1975).

The existence of a maximum in the angle β, a maximum which increases as separation is approached, suggests that the flow behaviour in the present case is analogous with that in the three-dimensional steady case. The main difference between steady

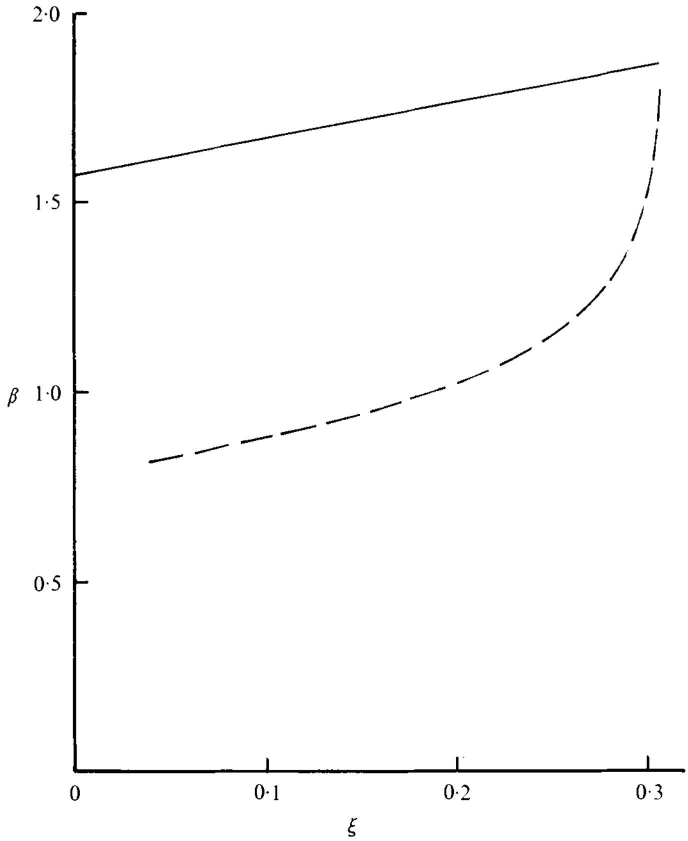

FIGURE 6. Variation of maximum flow deflexion angle β_{max} and angle β_s of local lines ξ = constant with ξ; $\alpha = 1$, $\overline{U} = \overline{V} = 0{\cdot}2$.

and unsteady flow appears to be that separation, which occurs at the wall in steady flow, occurs away from the wall in unsteady flow. If this is indeed true, the maximum value β_{max} of β in the boundary layer should approach the angle of the separation line as separation is approached. In the moving co-ordinate system, each line of constant ξ is given by

$$\xi = x^*/(1-\alpha y^*)$$

or, alternatively,

$$y^* = (1-x^*/\xi)/\alpha.$$

Thus the angle which each line of constant ξ makes with the x axis is given by

$$\beta_s = \arctan(-1/\xi\alpha).$$

Since separation occurs at a fixed value of ξ, say ξ_{sep}, the angle the separation line makes with the x axis is

$$\beta_{sep} = \arctan(-1/\xi_{sep}\,\alpha). \tag{22}$$

In figure 6 the values of β_{max} and β_s have been plotted as a function of ξ. If the value of ξ at the last station for which convergence is obtained is taken to be ξ_{sep}, then in the present case ($\alpha = 1$, $\overline{U} = \overline{V} = 0{\cdot}2$)

$$\beta_{sep} = \arctan(-1/0{\cdot}3062) = 1{\cdot}868.$$

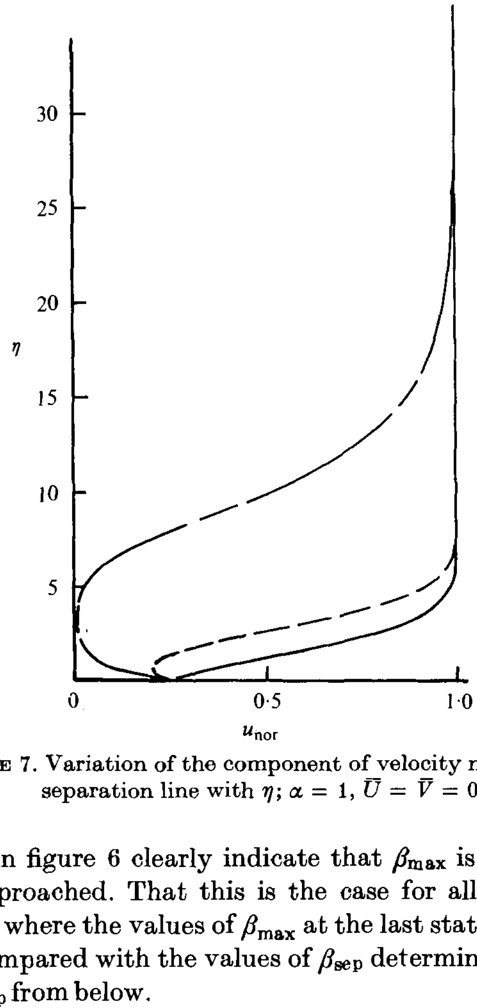

FIGURE 7. Variation of the component of velocity normal to the separation line with η; $\alpha = 1$, $\bar{U} = \bar{V} = 0{\cdot}2$.

The results shown in figure 6 clearly indicate that β_{max} is rapidly approaching β_{sep} as separation is approached. That this is the case for all the flows investigated is indicated in table 1, where the values of β_{max} at the last station for which convergence was obtained are compared with the values of β_{sep} determined from (22). In each case β_{max} approached β_{sep} from below.

Thus, in the moving co-ordinate system, the streamlines turn and approach a condition of tangency with the separation line. The angle $\bar{\beta}$ of the instantaneous streamlines in the fixed co-ordinate system is related to the corresponding angle β in the moving co-ordinate system by

$$\tan\bar{\beta} = \frac{\bar{v}}{\bar{u}} = \frac{1+V/(v_\delta G'(\xi,\eta))}{1+U/(u_\delta F'(\xi,\eta))}\tan\beta.$$

On the other hand, the angle β_{sep} of the separation line is the same in both the moving and the fixed co-ordinate system. Clearly, since the streamlines in the moving co-ordinate system become tangential to the separation line, the corresponding instantaneous streamlines in the fixed co-ordinate system cannot become tangential to the separation line. Separation is most easily identified, then, in the co-ordinate system moving with separation, as in the two-dimensional unsteady case.

It is interesting also to consider the effect of variations in the parameter α. For $\alpha = 0$, the flow corresponds to flow over an infinite cylinder with axis parallel to the x axis and separation occurs along a line parallel to the x axis, i.e. $\beta_{sep} = \frac{1}{2}\pi$. For $\alpha > 0$, there is flow reversal of the x component of velocity and separation occurs

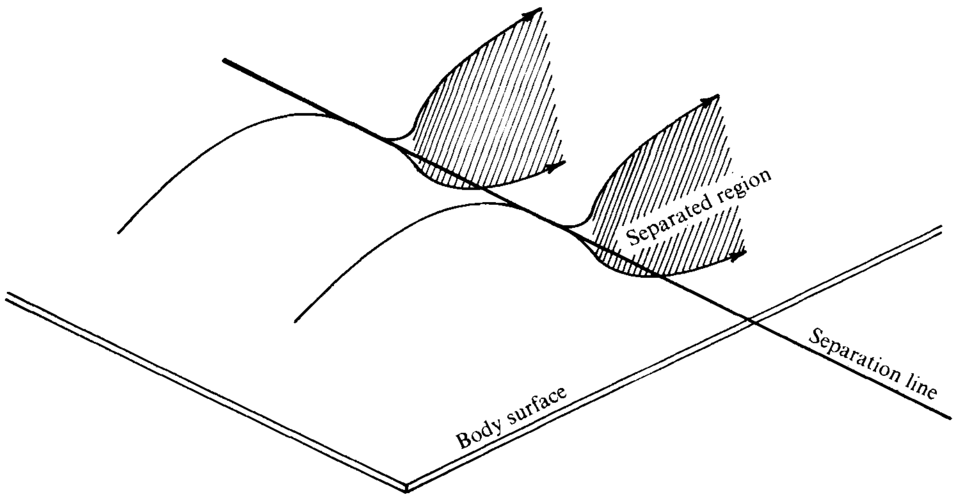

FIGURE 8. Graphical representation of unsteady three-dimensional boundary-layer separation.

along lines for which $\beta_{sep} > \frac{1}{2}\pi$, as described above. For $\alpha < 0$, the pressure gradient in the x direction is still positive (adverse), but the pressure gradient in the y direction is negative (favourable). As a result of this combination, the x component of velocity near the wall is decelerated while the y component of velocity near the wall is accelerated. Separation occurs in this case alone lines for which $\beta_{sep} < \frac{1}{2}\pi$, as indicated in table 1.

There is one additional check which may be made to verify the picture of unsteady three-dimensional separation which is emerging. If unsteady three-dimensional boundary-layer separation is characterized by the flow within the boundary layer turning to become tangential to the separation line at separation, as indicated above, then the velocity component normal to the separation line should approach zero at a point in the boundary layer as separation is approached. Figure 7 shows the variation of the normal component u_{nor} of velocity with η. Here, u_{nor} is given by

$$u_{nor} = (u_\delta^* F' \cos\beta_{sep} + v_\delta^* G' \sin\beta_{sep})/(u_\delta^* \cos\beta_{sep} + v_\delta^* \sin\beta_{sep}).$$

The normal component of velocity does indeed approach zero as separation

$$(\xi_{sep} \simeq 0{\cdot}3062)$$

is approached and the value of β_{max} and the minimum value of u_{nor} occur at the same value of η, as one might expect. The velocity profiles shown in figure 7 are quite similar to the velocity profiles in a co-ordinate system moving with separation in unsteady two-dimensional flow (Williams & Johnson 1974).

From the results obtained, a clear picture of unsteady three-dimensional boundary-layer separation has emerged, at least for the case of upstream-moving separation. In numerical solutions of the three-dimensional unsteady boundary-layer equations, separation is heralded by (i) a rapid increase in the number of iterations required to obtain converged solutions at each station and (ii) a rapid increase in the vertical component of velocity. Physically, separation is in this case characterized by the flow turning to become tangential to the separation line in a reference system moving with separation. The separation line in the unsteady case lies within the boundary layer, away from the wall, whereas the separation line in the steady case lies on the wall. This, then, is the three-dimensional generalization of the two-dimensional (Moore–Rott–Sears) model.

This description of unsteady three-dimensional boundary-layer separation has been obtained from numerical solutions of the boundary-layer equations, solutions which can only approach and never reach separation because of tne singular behaviour of the solutions close to separation. Nevertheless, it is not difficult to speculate on the physical nature of the flow along the separation line and just downstream of this line. Since the flow along the separation line is tangential to the separation line while there is flow normal to the separation line both above and below it, the separation line must represent the front of a bubble-like structure which is embedded within the flow. Figure 8 depicts such a structure. Streamlines which become part of the separation line originate upstream and approach the separation line. These streamlines become tangential to the separation line, so that the separation line is an envelope of all of these streamlines. Eventually, each streamline splits so that part of the flow passes over and part of the flow passes under the separated region as indicated in figure 8. Figure 8 may be considered as a graphical representation of the flow in the moving co-ordinate system, in which, in the present analysis, the flow is steady.

REFERENCES

Blottner, F. G. 1970 Finite-difference methods of solution of the boundary layer equations. *A.I.A.A. J.* **8**, 193.

Maskell, E. C. 1955 Flow separation in three-dimensions. *R.A.E. Rep. Aero.* no. 2565.

Peake, D. J., Rainbird, W. J. & Atraghji, E. G. 1972 Three-dimensional flow separation on aircraft and missiles. *A.I.A.A. J.* **10**, 567.

Sears, W. R. 1948 The boundary layer on yawed cylinders. *J. Aero. Sci.* **15**, 49.

Sears, W. R. & Telionis, D. P. 1975 Boundary layer separation in unsteady flow. *SIAM J. Appl. Math.* **28**, 215.

Telionis, D. P. 1975 Calculation of time dependent boundary layers. *Unsteady Aerodynamics. Proc. Symp. Univ. Arizona*, p. 155.

Tsahalis, D. T. 1977 Laminar boundary layer separation from an upstream moving wall. *A.I.A.A. J.* **15**, 561.

Williams, J. C. 1975 Semisimilar solutions to the three-dimensional laminar boundary layer. *Appl. Sci. Res.* **31**, 161.

Williams, J. C. 1977 Incompressible laminar boundary layer separation. *Ann. Rev. Fluid Mech.* **9**, 113.

Williams, J. C. & Johnson, W. D. 1974 Semisimilar solutions to unsteady boundary layer flows including separation. *A.I.A.A. J.* **12**, 1388.